EPJ Web of Conferences **9**, 83–94 (2010)
DOI: 10.1051/epjconf/201009006

Radiative effects of the cloudy atmosphere from ground and satellite based observations

A. Macke[1], J. Kalisch[2], Y. Zoll[2], and K. Bumke[2]

[1] Leibniz-Institute of Tropospheric Research, 04318 Leipzig, Germany
[2] Leibniz-Institute of Marine Sciences, 43105 Kiel, Germany

Abstract. The radiation budget from surface observations and parameterizations is combined with that from satellite observations along the cruise tracks of the German icebreaker POLARSTERN in the North and South Atlantic under tropical, subtropical and mid-latitude conditions. Between 2008 and 2010 The German Leibniz-network OCEANET participated in six transfers from or to Bremerhaven, Germany to or from Punta Arenas, Southern Chile or Cape Town, South Africa. The present chapter introduces exemplarily the atmospheric measurements and resulting radiation products. The following properties are derived: Standard meteorological data, broadband downward solar and thermal irradiances, underwater profiles of spectral irradiance, latent and sensible heat fluxes, humidity and temperature profiles, water vapour and liquid water path, aerosol optical thickness and vertical profiles of aerosol optical thickness, cloud cover and cloud type. Cloud radiative effects at the surface have been determined for different marine cloud types. Together with top-of-atmosphere radiation fluxes from the SEVIRI radiometer onboard METEOSAT, the effect of clouds on atmospheric heating or cooling have been determined. The resulting cloud/radiation correlations will help to quantify the effects of clouds on the surface, ToA- and atmospheric radiation budget and to evaluate the ability of climate models to simulate these effects.

1 Introduction

Clouds are an impressive manifestation of complex dynamical-thermodynamical processes in the atmosphere. They influence our weather and climate and they are affected by anthropogenic climate changes at the same time. With a global coverage of more than 60% clouds have a prevailing effect on the radiation budget of our planet. Latent heat from condensation processes helps driving atmospheric circulation cells, which in turn interact with the ocean system (e.g. ENSO). (Negative) latent heat is transported by cloud related condensation and evaporation processes, and the corresponding transports of fresh water determine vegetation over land and the stability of the oceanic boundary layer.

This well recognized significance of the cloudy atmosphere on the state of the earth's climate stands in strong contrast to our quantitative understanding of the relevant physical processes in clouds. The reasons for this are 1) the complex macro- and microphysical properties of clouds, 2) their fast temporal development, and 3) their difficult experimental accessibility. For example, it is well known that the global cloud albedo effect dominates the global cloud greenhouse effect, thus clouds are cooling our climate system [1]. However, estimations of the global mean value of this so-called net radiative forcing (see further down for the exact definition) range from -18 to $-30\,\mathrm{Wm}^{-2}$ [2] depending on

the method and time of observation. The uncertainties are much larger at local scales and for specific cloud types.

According to the IPCC report "Climate Change 2001" [3] the increase of CO_2 from 1750 until today produces with $+1.4\,\mathrm{Wm}^{-2}$ the largest anthropogenically induced change in the global radiative forcing. Comparing this number with the uncertainties of about $20\,\mathrm{Wm}^{-2}$ in cloud radiative forcing clearly demonstrates that a reasonable exploration and prediction of our climate system requires an improved understanding of cloud-radiation interactions. Pure model based estimations of the cloud radiative effects are highly uncertain, as large-scale models do not resolve the cloud structures that are relevant for radiative processes. A typical grid cell size of a global circulation model is of the order of 100 km whereas the distance between two scattering events inside a cloud is around 100 m. Thus, simultaneous observations of cloud physical and radiative properties are required to obtain realistic cloud-radiative forcings.

As the German Research Vessel POLARSTERN is mostly operating under summer polar conditions in both the Arctic and in the Antarctic, the resulting transfer routes between Germany and either South America or South Africa provide an excellent opportunity to perform atmospheric and oceanic observations under tropical, subtropical and mid-latitude conditions in both hemispheres.

A lucky coincidence results from the fact that the European weather satellite Meteosat "sees" the major part of the Atlantic Ocean where the ship observations are performed so that collocated satellite data provide matching ToA radiative fluxes.

The transfer of energy and material between atmosphere and ocean is a key in understanding climate processes. The corresponding fluxes of radiation, heat, water vapour, and CO_2 are driven by the local composition of the upper ocean and the troposphere. Clouds and aerosol (directly and indirectly via cloud processes) mostly determine the surface radiation budget, which in turn is the major part of the surface energy budget. Regional and large-scale patterns of the energy budget produce the dynamical forcing for cloud evolution. This complex interplay between clouds and energy budgets is recognised as the largest source for uncertainties in understanding climate processes [4].

The aim of this chapter is to demonstrate the effect of clouds on our radiation budget at the surface and at the top of atmosphere based on observations. In the framework of the German Leibniz-Programme OCEANET a large number of measurements have been carried out on board POLARSTERN. Prior to the OCEANET project, the Atlantic traverses of the polar research vessels ACADEMICIAN VAVILOV and ACADEMICIAN IOFFE in 2004 to 2006 as well as the POLARSTERN Atlantic traverses in 2007 have been used in the framework of the Meridional Ocean Radiation Experiment MORE [5,6]. From 2008 to 2010 all Atlantic traverses of POLARSTERN have been taken advantage of in the OCEANET project. Furthermore, a reduced set of OCEANET observations (mostly radiation and cloud imager) have been carried out under sea ice conditions in the Arctic and the Antarctic Ocean. Figure 1 shows all OCEANET and OCEANET-related cruises.

A detailed description of all measurements performed during the OCEANET cruises can be found in the POLARSTERN cruise reports [7,8].

2 Atmospheric measurement devices

Figure 2 shows the OCEANET observatory container on the observatory deck in 20 m height above sea level with turbulent flux mast, standard meteorology, lidar hatch, pyrano- and pyrgeometer, sky imager, and microwave radiometer. The larger weather proved frontal part contains a lidar and all data acquisition devices. The back part contains a hatch for the microwave radiometer and additional upward looking devices.

Fluxes of sensible and latent heat are derived from a fast responding absorption hygrometer (LICOR 7500) for humidity measurements with 30 Hz temporal resolution in combination with a sonic anemometer (METEK USA-1) for wind measurements with 10 Hz resolution. The inertial dissipation method [9,10] is applied to obtain the turbulent fluxes, as it is insensitive against ship movements. The Scalable Automatic Weather Station SCAWS (see [8]) developed at the DWD is used to obtain wind, pressure, temperature, humidity, shortwave and longwave downward radiation (DSR, DLR) as well as position. The data are taken every second.

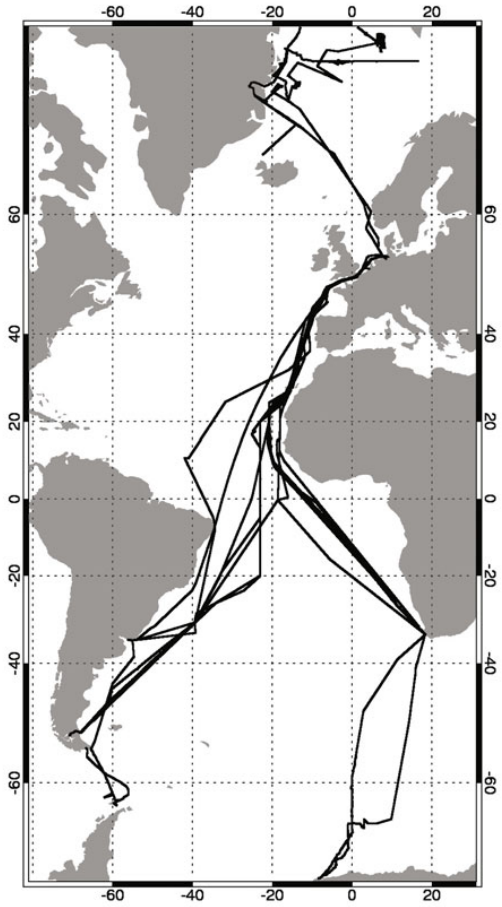

Fig. 1. Cruise tracks of research vessels ACADEMICIAN IOFFE, ACADEMICIAN VAVILOV and POLARSTERN that have been used for cloud and radiation measurements between 2004 and 2009.

DSR is measured with a Kipp&Zonen CMP21 pyranometer, DLR with a Kipp&Zonen CGR4 pyrgeometer. Despite a 95% relaxation time of 5 seconds for the pyranometer and 18 seconds for the pyrgeometer data are sampled with 1 Hz resolution.

A full sky imager developed at IFM-GEOMAR [11] determines cloud cover and direct sun conditions as well as cloud type [12] every 15 seconds. Sky images are also used for detection of instrument shadowing by the ships super structure or other error sources.

The Humidity And Temperature PROfiler HATPRO by Radiometer Physics measures downward nadir microwaves at 14 channels around the 20–30 GHz water vapour absorption band (7 channels) and the 60 GHz oxygen absorption complex (7 channels) [13]. A modified version of the algorithm by [14] is used to convert the data to liquid water path (LWP) for warm non-precipitating clouds, to water vapor path (WVP, or Integrated Water Vapor IWV) as well as to profiles of temperature and humidity.

The POLLY-XT multiwavelength Raman lidar [15] is used to obtain profiles of aerosol extinction coefficient and aerosol microphysical properties.

Auxiliary data like aerosol optical thickness from a MICROTOPS sun photometer [16], spectral UV irradiance (see description in [8]), and downward visible irradiance down to 150 m below sea surface round out the data suite.

Major additions to the ship data are the SEVIRI solar and thermal radiances taken onboard the geostationary METEOSAT Second Generation satellites. With 15 minutes temporal and 1–3 km

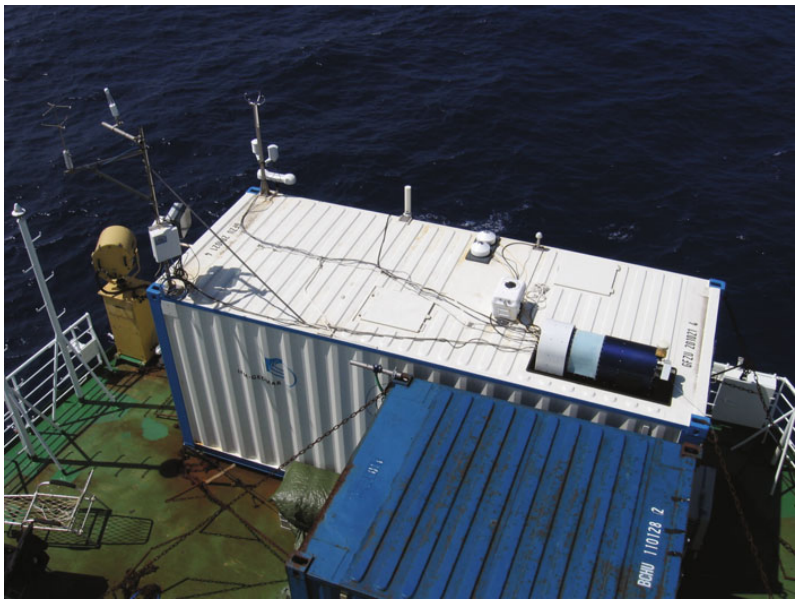

Fig. 2. The OCEANET sea container (white 20 feet container with frontal part to the left) on the observatory deck onboard POLARSTERN with turbulent flux tower (front-left), standard meteorology (front-right), lidar hatch (middle-left), pyrano- and pyrgeometer (middle right), sky imager (middle) and microwave radiometer (back-left). Photograph by Henry Kleta.

spatial resolution and a coverage of the Atlantic Ocean from 60° south to 60° north almost the entire Atlantic transfer cruises of POLARSTERN are accompanied by the satellite data. The SEVIRI data provide cloud cover, cloud type, cloud optical thickness and droplet effective radius as well as Top Of Atmosphere (TOA) shortwave and longwave upward fluxes.

3 Atmospheric composition

In the following, a brief overview of the atmospheric remote sensing products is given. The HATPRO microwave radiometer provides the water vapor path WVP under all-sky conditions as well as the liquid water path LWP for warm (meaning no ice phase) non-precipitating clouds. The 14 channels also allow inferring vertical profiles of humidity and temperature. Figure 3 shows WVP and LWP from the HATPRO microwave radiometer during the POLARSTERN cruise ANT-XXVI/1 (fall 2009) as a function of latitude. The red triangles in the upper IWV-plot denote the in-situ observed IWV from radiosondes. The vertically integrated water vapour ranges from 10 kgm^{-2} in dry subtropical regions to more than 60 kgm^{-2} in the Inner Tropical Convergence Zone ITCZ, where water vapor is lifted up to 18 km height. The comparison with the true IWV from occasional radiosoundings demonstrates a generally good agreement. The drift of the radiosonde during its ascent may cause some deviations. The vertically integrated condensed water reaches 2000 gm^{-2} for deep convection thunderstorm clouds in the ITCZ. However, the HATPRO retrieval is reliable for water clouds with LWP smaller than 500 gm^{-2} so that these large values must be regarded with care. Because of the lack of in-situ LWP a direct validation similar to that for the IWV is not possible. However, cases of 0 LWP can easily be identified by means of sky imager so that at least a single point calibration is possible. It is of interest to note that the amount of condensed water in the atmosphere is roughly 100 times smaller than the water vapour. Still, the scattering of solar radiation and re-emission of thermal radiation by cloud droplets has a much larger effect on the radiation budget than the natural green house effect due to the presence of water vapour.

The necessary condition for cloud particles to form is sufficient amount of water vapour (supersaturation) and the presence of aerosol particles that serve as condensation nuclei. A certain background

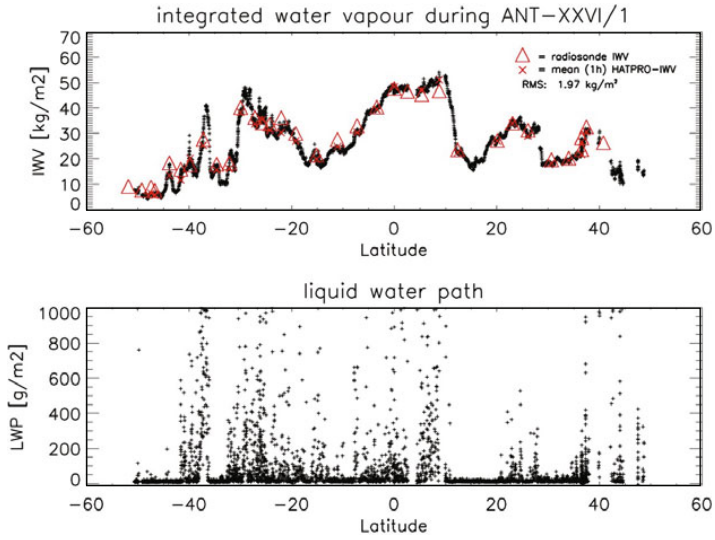

Fig. 3. IWV and LWP from the HATPRO microwave radiometer during the POLARSTERN cruise ANT-XXVI/1 (fall 2009) as a function of latitude. The red triangles in the IWV-plot denote the in-situ observed IWV from radiosondes.

aerosol lead is always present, under marine conditions mostly in the form of dried sea spray. But there exists a huge variety of additional aerosol species with different inorganic and organic chemical compositions. These aerosol species can either form by gas to particle conversions locally or they are advected from remote sources. Largest natural aerosol loads in the atmosphere result from biomass burning, volcanic eruptions and from strong winds over deserts, which lift and transport huge amounts of mineral dust. The latter has been observed during the POLARSTERN cruise ANT-XXVI/1 during fall 2009 near the Cape Verde Islands. Figure 4 shows the backscatter profile of the IfT POLLY-XT lidar during the passage below a Saharan dust Storm event. The reddish colours nicely show the structured dust plume between 1000 and 2000 m height. These events have a significant effect on the solar and thermal radiation budget. The optical thickness of the dusty atmosphere exceeds 0.7 during this event. Typical values for marine clear sky optical thickness are around 0.1. Note that the optical thickness of water clouds is mostly larger than 10, which emphasizes the dominant role of clouds on the radiation budget. However, as the size and lifetime of cloud droplets depends on the physical and chemical compositions of the cloud condensation nuclei, aerosol has a strong indirect effect on the radiation budget of our planet [17].

4 Cloud induced radiation enhancement

The effect of clouds on the surface radiation budget is a net cooling. Clouds reflect sun light back to space (with a global mean albedo of 0.5). Clouds absorb about 15% of the incoming solar radiation (see Fig. 6 and description in the following section). Thus, less radiation reaches the surface in the presence of clouds compared to clear-sky situations. However, locally and for short time periods clouds can substantially enhance the solar irradiance at the surface. This well known and so-called “broken-cloud effect” results from enhanced downward radiances from the sky outside the solar disk by the usually white cumulus type clouds (see e.g. [18]). This diffuse contribution is much larger than that from the blue clear sky. Largest broken-cloud effects occur under nearly overcast conditions whenever the full solar disk shines through a cloud gap, and the strong forward scattering cloud droplets produce a strong beam of diffuse sunlight surrounding the sun. Figure 5 shows shows the diurnal cycle of the donwelling solar radiation in units of Wm^{-2} for the 9^{th} of November 2009 measured onboard POLARSTERN during the cruise ANT-XXVI/1. At this day, the solar radiative flux reached 1647 Wm^{-2}, the largest ever observed value for all POLARSTERN cruises so far. The diagram also shows the sky image during the time of the maximum radiation. Although the direct solar disk is not detectable one can nicely see

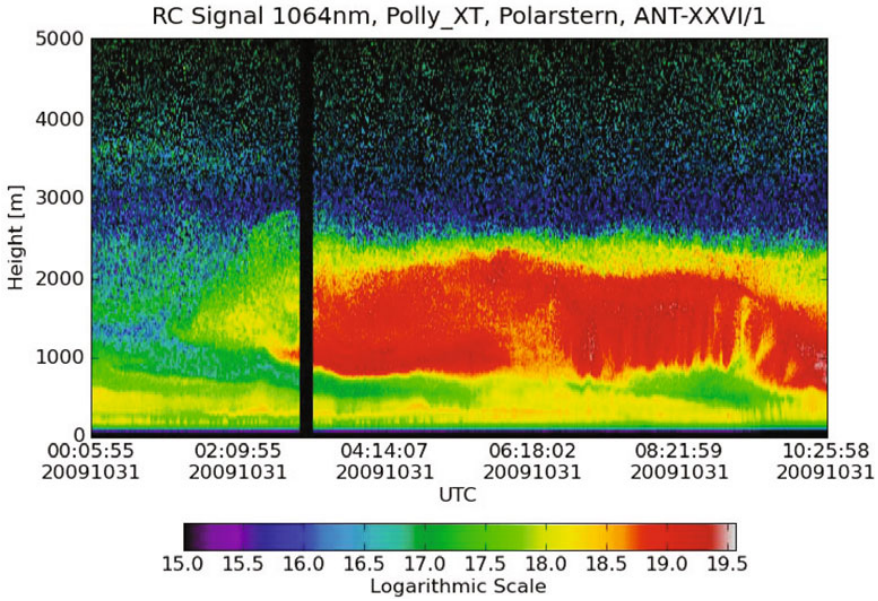

Fig. 4. Backscatter profile of the POLLY-XT lidar during the passage below a Saharan dust Storm event. Diagram by Thomas Kanitz.

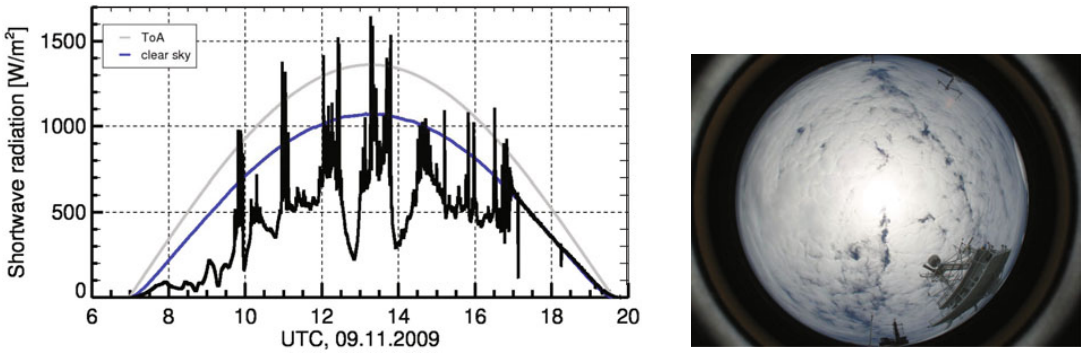

Fig. 5. Diurnal cycle of downward solar radiation at the surface measured during the POLARSTERN cruise ANT-XXVI/1 in fall 2009 together with a the radiative flux arriving at the ToA and at the surface under clear sky conditions. The sky image at the time of largest incoming radiation is shown as well.

the strong enhancement of the downward diffuse radiance around the disk. Note that the solar radiative flux at the top of the atmosphere and with perpendicular incidence is 1367 Wm^{-2} (denoted as solar constant). Thus, the strong forward scattering by cloud droplets – most effective in the vicinity of the sun – can result in atmospheric transmissivities considerably larger than 1, at least for short times. Typical durations of largest radiation enhancements are a few seconds [18].

5 Radiation budget

Figure 6 shows some estimates of the global mean shortwave radiation budget from a combination of observations and models [19], from the ECHAM climate mode, and from a specific modification of the ECHAM model that accounts for 3d radiative transfer effects [20], which its denoted as SP for "Schewski Parameterization". There are large differences between models due to different treatment

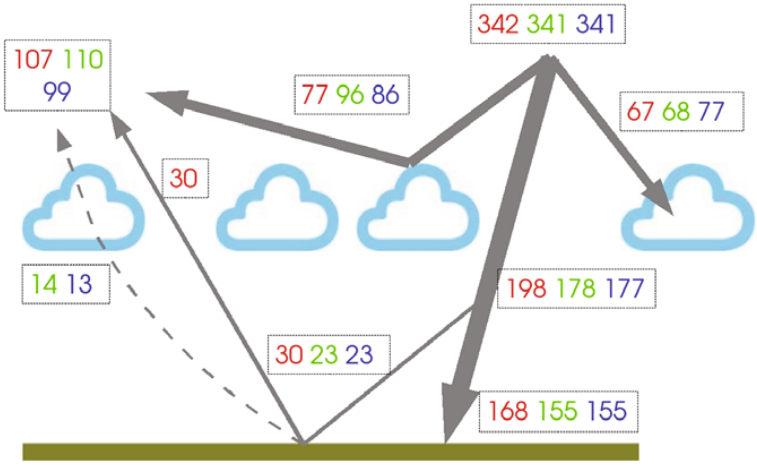

Fig. 6. Global annual mean SW energy budget from [19], ECHAM5 and SP. Units are Wm^{-2}. The dashed array indicates that the SW radiation reflected at the surface for ECHAM5. Diagramm by [24].

of cloud radiative transfer and due to the different spatial and temporal distributions within the model results.

We use the following nomenclature for radiation fluxes: DSR = Downward Shortwave Radiation; OSR = Outgoing Shortwave Radiation; DLR = Downward Longwave Radiation; OLR = Outgoing Longwave Radiation. The radiation budget is defined by downward minus upward quantities. The net radiation budget is the sum of shortwave and longwave budget. The upward shortwave radiation is calculated from a solar zenith angle dependent ocean surface albedo according to Fresnels law of reflection multiplied by the insolation.

Figure 7 shows the shortwave, longwave and total radiation budget at the surface measured along the POLARSTERN cruise ANT-XXVI/1 as a function of latitude from south (negative values) to north (positive values). Black dots denote daily means. Because of the low and only slightly changing surface albedo the shortwave budget is dominated by the sun elevation with the corresponding diurnal cycle. By definition, the daily mean shortwave budget is always positive. The longwave radiation budget results from a gain of thermal radiation from the atmosphere and a loss of thermal emission from the surface. The radiation fluxes are determined by the emissivity and temperature of atmosphere and surface. Especially over ocean the temperature is not significantly varying with the solar elevation (no heating of the surface or the atmosphere during the day). Fluctuations of the longwave budget result mostly from changes in cloud cover and cloud bottom height (and thus cloud bottom temperature). In fact, the downward thermal radiation from the atmosphere can be used to estimate cloud cover [21]. Because the Atlantic transfer mostly experienced subtropical and tropical conditions, the solar budget was in most cases much larger than the thermal budget and the net budget shows the same diurnal cycles as the shortwave one. Also, the net radiation budget at the surface was mostly positive meaning that the radiation gain at the surface was larger than the thermal loss. In Polar Regions with small solar radiation and small thermal re-emission from the colder atmosphere, the net radiation budget is negative. On global average, the radiation gain at the surface is larger than the radiation loss due to the greenhouse effect of clouds and atmosphere. The difference is compensated by latent and sensible heat fluxes.

While surface sites immediately allow measuring the downward or upward flux into the corresponding upper or lower hemisphere, satellite based radiometer only measure radiances that are reflected or emitted from a certain field of view into the viewing direction of the radiometer. In the present study we take advantage of the spectral reflected solar and emitted thermal radiances from the atmosphere as measured by the SEVIRI radiometer onboard the geostationary satellite METEOSAT. By means of narrow-to-broadband [22] and radiance-to-flux conversions [23] the observed radiances can be converted into outgoing shortwave and outgoing longwave radiation fluxes at the ToA. Both conversions depend on the satellite viewing angle, the position of the sun, the bidirectional

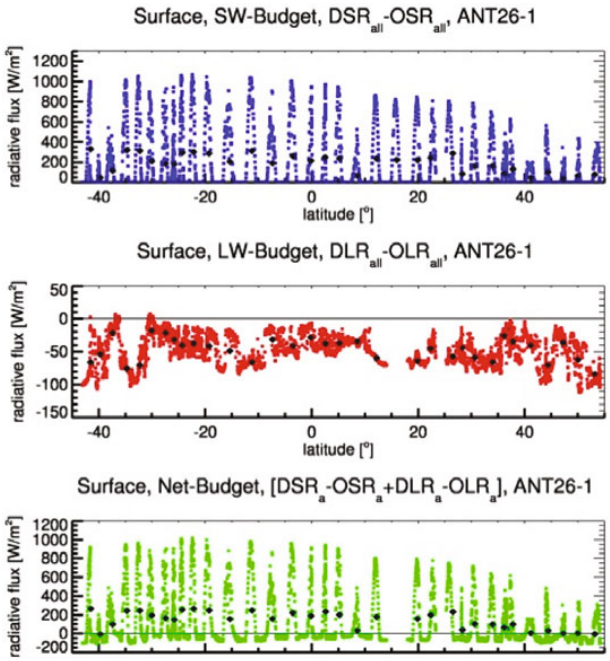

Fig. 7. Shortwave (top), longwave (middle) and net radiation budget at the surface as a function of latitude during POLARSTERN cruise ANT-XXVI/1. The black dots denote daily means.

reflection/emission function of the surface. The latter depend on the surface type, cloud cover and cloud type. Errors in the scene identification can cause corresponding errors in the ToA radiative fluxes. Much work has been invested in determining radiative fluxes both at the surface and at the ToA from satellite measurements. In the present paper, the algorithms by [22,23] iareused to obtain the ToA fluxes from the Meteosat spectral radiance data.

Figure 8 again shows the shortwave, longwave and total radiation budget at the Top of the Atmosphere (ToA) measured along the POLARSTERN cruise ANT-XXVI/1 as a function of latitude from south (negative values) to north (positive values). The shortwave budget is dominated by the diurnal variation of the solar elevation, the thermal budget by the occurrence of warm strongly emitting clear-sky ocean surfaces. Small (negative) values of the thermal loss are associated with the presence of cold high clouds. The net (shortwave plus longwave) ToA radiation budget is dominated by the shortwave part owing to the subtropical and tropical conditions. At Polar Regions, the longwave emission overtops the shortwave gain. In contrast to the surface the global mean ToA radiation budget is close to zero because the Earth as a thermodynamic system always tries to reach radiation equilibrium. However, longterm transports of heat in the ocean or latent heat storage in the cryosphere can lead to small deviations from this equilbrium.

The daily mean shortwave and longwave radiation budget at the ToA is very large (several $100\,\mathrm{Wm}^{-2}$). Still, the net budget is closer to zero, indicating that the thermodynamic systems mentioned above partly succeeds also locally to come close to equilibrium. Interestingly, the net budget in the ITCZ with its persistent belt of Cb clouds is nearly zero. Obviously, the reduced gain of solar radiation due to strong reflection is nearly balanced by the reduced loss of thermal radiation by the cold cloud tops.

6 Cloud radiative effect

As briefly indicated in the previous section, clouds affect the radiation budget in two opposing ways. At the surface the reduction of solar radiation during the day fights with the gain of thermal emission during day and night. Similarly, the increased reflection of solar radiation by clouds may be partly

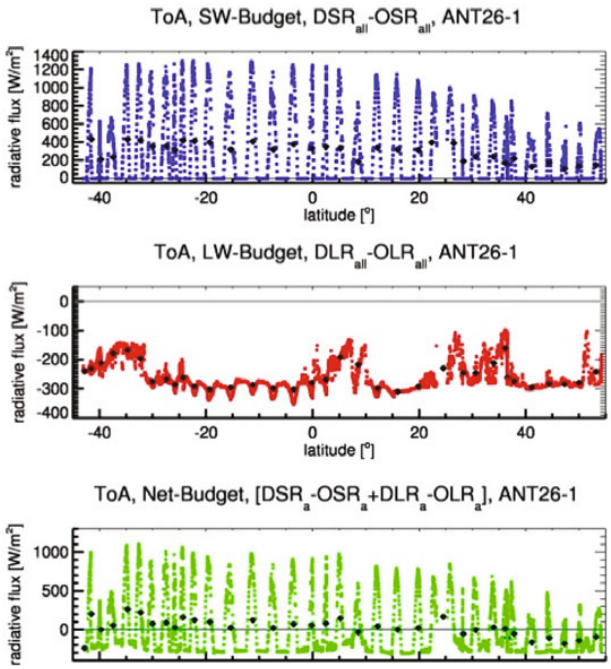

Fig. 8. Shortwave (top), longwave (middle) and net radiation budget at the surface as a function of latitude during POLARSTERN cruise ANT-XXVI/1. The black dots denote daily means.

(or over-) compensated by reduced emission of the colder cloud tops. Thus, it is not obvious wether clouds lead to a net gain or loss in the total amount of radiation compared to clear skies.

This effect of clouds on the radiation budget is usually quantified by the difference in the radiation fluxes between all-sky and clear-sky conditions and is denoted as cloud radiative effect.

By definition the CRE at clear-sky conditions must be zero. However, errors in determining clear-sky radiation may cause deviations from this theoretical value. While the radiation fluxes under all-sky conditions are directly observable, the clear-sky references must be taken either from nearby clear-sky situations or from parameterizations. In most cases, a nearby clear-sky situation is not available and parameterizations are commonly used. In this work, we take the clear-sky downward shortwave radiation from a parameterization by [25] optimized for marine conditions by [11]. In addition to the solar elevation, the parameterization basically accounts for water vapour absorption by taking the observed humidity and temperature at the surface into account. Together, these two values are strongly correlated with the integrated water vapour under clear sky conditions. For the downward clear-sky thermal radiation at the surface the parameterization by [26] is used, which only requires surface air temperature as input parameter.

Figure 9 shows the shortwave, longwave, and net cloud radiative effect at the surface. Compared to clear-skies, clouds mostly block the sun and lead to a reduction (negative CRE) in the radiation. The shortwave CRE can be as large as 900 Wm^{-2} when large Cb clouds completely blocks the direct and large parts of the diffuse solar radiation at highest sun elevations. The frequently occurring broken-cloud-effect cases (see section 4) result in positive CREs, i.e. a radiation enhancement due to the presence of clouds. Clearly, the blocking effect is much larger than the enhancement effect. In the longwave spectrum, clouds always increase the amount of downward radiation (positive CRE) compared to clear skies.

Note that some scatter around the CRE = 0 line is most likely due to errors in the parameterizations of the clear sky references.

Finally, the cloud radiative effect at the ToA and for the atmospheric column along the ship cruises is shown in Figs. 10 and 11, respectively. The column CRE is is given by the sum of surface CRE

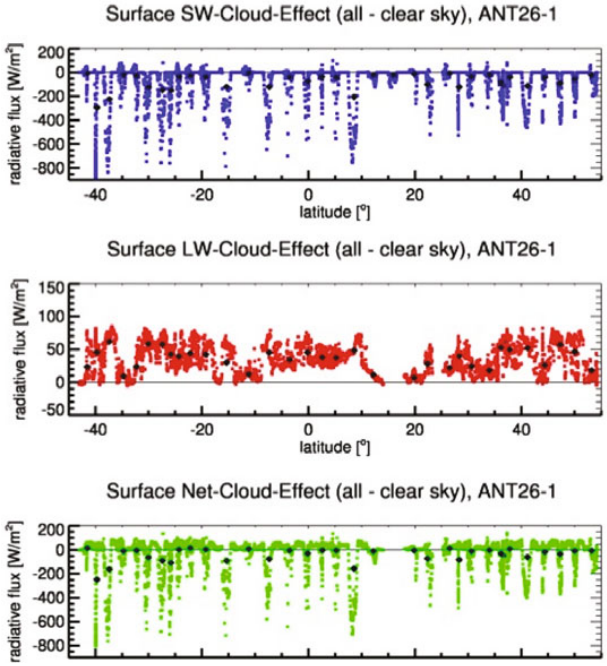

Fig. 9. Shortwave (top), longwave (middle) and net cloud radiative effect at the surface as a function of latitude during POLARSTERN cruise ANT-XXVI/1. The black dots denote daily means.

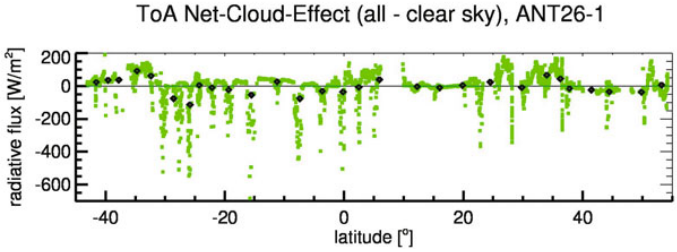

Fig. 10. Net cloud radiative effect at the top of the Atmsophere as a function of latitude during POLARSTERN cruise ANT-XXVI/1. The black dots denote daily means.

and the ToA CRE and describes to what extend the presence of clouds leads to a net gain or loss of radiation compared to a clear sky atmosphere.

High and optically thin clouds like cirrus or alto cumulus are semi-transparent in the solar spectrum so that a large portion of the solar irradiance can enter the atmosphere/surface system despite the presence of clouds. On the other hand, these clouds emit much less thermal radiation at their cloud tops so that these clouds increase the amount of available radiation energy. In contrast to this situation, low water clouds reflect much of the solar radiation back to space but are not much colder than the ocean surface so that these clouds have a cooling effect at the ToA. Figure 10 shows both positive and negative CRE along the ship cruise with no significant meridional dependency. The correlation of the observed CRE with observed dominant cloud types is ongoing work.

Several competing mechanisms determine magnitude and sign of the CRE for the atmospheric column. Clouds absorb solar and thermal energy, which implies that the presence of clouds leads to a radiation gain. However, a reduced surface warming due to clouds reduces the thermal emission into the atmosphere, which is more effectively absorbed than the solar radiation (the latter being mostly scattered). Also, bright low-level clouds lead to larger path lengths of solar photons, which are

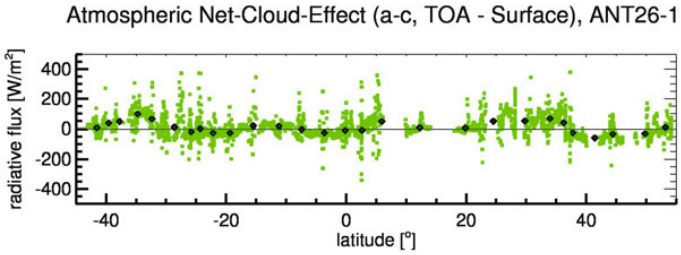

Fig. 11. Columnar cloud radiative effect for the atmospheric column as a function of latitude during POLARSTERN cruise ANT-XXVI/1. The black dots denote daily means.

otherwise absorbed at the ocean surface. The atmospheric CRE (Fig. 11) indeed shows both a warming and a cooling behaviour, and is stronger correlated to the CRE at the ToA than at the surface.

Current research is investigating the effect of cloud types, cloud physical properties (LWP, cloud bottom height, ...), solar elevation among others on the cloud radiative effect at the surface, at the ToA and for the atmospheric column. Furthermore, solar and thermal radiative fluxes from radiative transfer simulations with observed cloud properties as input parameters are currently compared to observations.

7 Conclusions

The aim of this chapter was to introduce the concept of the cloud radiative effect as an important driver of the energy budget of our climate system. The combination of meridional ship based surface radiation budget observations with ToA radiation budget from co-located satellite data provides an excellent opportunity to capture the cloud radiative effect for different climate zones and weather conditions. Five years of data have been collected during the Atlantic Ocean transfer cruises of the Russian research vessels ACADEMICIAN IOFFE and ACADEMICIAN VAVILOV as well as the German research vessel POLARSTERN. Both the observations and the data analysis will continue for several years. In the end, we hope to arrive at robust numbers of true CREs for different cloud types, solar illumination conditions, daily means, cloud thickness and cloud liquid water path among other parameters. Due to the huge spatial and temporal complexity of clouds a realistic simulation of cloud radiative effects is beyond the capabilities of climate models. However, climate model cloud-radiation fields to observations may provide a significant step in global climate modelling.

The authors are grateful to the Alfred-Wegener-Institute for the opportunity to perform measurements during the Atlantic transfer cruises ANT-XXIII/10, ANT-XXIV/1, ANT-XXIV/4, ANT-XXV/1, ANT-XXV/2, ANT-XXV/5, ANT-XXVI/1, ANT-XXVI/4 of RV POLARSTERN, and to the Shirshov Institute for participating in the Atlantic transfer cruises of RV ACADEMICIAN VAVILOV and RV ACADEMICIAN IOFFE from 2004 to 2006.

References

1. B.A. Wielicki, R.D. Cess, M.D. King, D.A. Randall, E.F. Harrison, BAMS, **76**(11), 2125–2153 (1995)
2. V. Ramanathan, R.D. Cess, E.F. Harrison, P. Minnis, B.R. Barkstrom, E. Ahmad, D. Hartmann, Science, **243**, 57–63 (1989)
3. J.T. Houghton, Y. Ding, D.J. Griggs, M. Nouger, P.J. van der Linden, X. Dai, K. Maskell, and D. Xiaosu, Climate Change 2001 - The Science of Climate Change: Contributions of Working Group I to the third Assessment Report of the Intergovernmental Panel on Climate Change (IPCC), Cambridge University Press (2001), p 881

4. IPCC *2007: The Physical Science Basis. Contribution of Working Group I to the Fourth Assessment Report of the Intergovernmental Panel on Climate Change* [Solomon S., D. Qin, M. Manning, Z. Chen, M. Marquis, K.B. Averyt, M.Tignor and H.L. Miller (eds.)]. Cambridge University Press, Cambridge, United Kingdom and New York, NY, USA (2007)
5. A. Sinitsyn, S. Gulev, A. Macke, J. Kalisch, S. Sokov, S. MORE cruises launched, Flux News, **1**, 11–13, (2006)
6. A. Macke, J. Kalisch, A. Sinitsyn, Alexei, A. Wassmann, More of MORE: the first MORE cruise onboard RV Polarstern. Flux News 4, 21–22 (2007)
7. A. Macke (Ed.) The expedition of the research vessel "Polarstern" to the Antarctic in 2008 (ANT-XXIV/4). Bremerhaven: AWI, 2009 (Reports on polar and marine research, **591**, (2009), 64 p
8. S. El Naggar, A. Macke, A. (Eds), The expedition of the research vessel "POLARSTERN" to the Antarctic in 2009 (ANT-XXVI/1), Bremerhaven: AWI, Reports on polar and marine research, **614**, (2010), p 79
9. C.W. Fairall and S.E. Larson, Boundary-Layer Meteorology, 34(3), 287–301 (1985)
10. S.D. Smith,. J. Geophys. Res., **93** ((C12),) 15467–15472 (1988)
11. J. Kalisch, A. Macke, Met. Zeit., 17(5), 603–611 (2008)
12. A. Heinle, A. Macke, A. Srivastav, Atmos. Meas. Tech., **3**, 557–567 (2010)
13. T. Rose, S. Crewell, U. Löhnert, C. Simmer, Atmos. Res., **75**(3), 183–200 (2005)
14. S. Crewell, U. Löhnert, RADIO SCIENCE, 38(3) (2003)
15. D. Althausen, R. Engelmann, H. Baars, B. Heese, A. Ansmann, D. Müller, M. Komppula, *J. Atmos. Oceanic Technol.*, **26**, 2366–2378 (2009)
16. A. Smirnov et al., J. Geophys. Res., 114, (2009)
17. J. Heintzenber, R.J. Chalrosn (Eds.), Clouds in the Perturbed Climate System, The MIT Press, 597p (2008)
18. N.H. Schade, A. Macke, H. Sandmann, C. Stick, Met. Zeit. 16(3), (2007)
19. Kiehl, J. und Trenberth, K.E., 1997: Earth's Annual Global Mean Energy Budget. Bull. Amer. Meteor. Soc., 78(2), 197–208
20. M. Schewski, A. Macke, Meteor. Z., **12**(6), 293–299 (2003)
21. B. Dürr, R. Philipona, JGR, **109** (2004)
22. N. Clerbaux, S. Dewitte, RMIB GERB Processing - SEVIRI Processing: Angular Dependency Models. RMIB technical Report, MSG-RMIB-GE-TN-8 (2002)
23. N. Clerbaux, S. Dewitte, RMIB GERB Processing - SEVIRI Processing: Spectral Modelling. RMIB technical Report, MSG-RMIB-GE-TN-5 (2002b)
24. S. Wahl, A. Macke, Application of 3D radiative flux parameterizations int he AGCM ECHAM5, 12th AMS Conference on Radiation, Madison, Wi, USA 2006 (poster available from `macke@tropos.de`)
25. J. Zillman, A study of some aspects of the radiation and heat budgets of the Southern Hemisphere oceans. Meteor. Stud. No. 26, Bureau of Meteorology, Canberra, 526 pp (1972)
26. S.B. Idso, R. D. Jackson, JGR, 74(23) 5397–5403 (1969)